

## Evaluation of torsional stiffness in beam and slab bridge decks based on load testing

I. Štimac Grandić<sup>1,\*</sup>, D. Grandić<sup>1</sup>, A. Bjelanović<sup>1</sup>

Received: October 2013, Accepted: September 2014

### Abstract

*In this paper, evaluation of torsional stiffness in beam and slab bridge deck elements is presented. A beam and slab bridge decks structurally behave as a grillage. A grillage has an efficient transverse load distribution due to transverse asymmetric load. In the case of bridge deck without transverse beams in the span, transverse load distribution depends on the torsional stiffness of longitudinal beams, transverse beams over the supports and deck slab. The results of load testing conducted on series of bridges in Croatia are compared with results obtained on different numerical grillage models in which torsional stiffness of main structural elements was varied. Five different numerical models for each tested bridge are used. To evaluate torsional stiffness of main structural elements of the bridge the transverse distribution coefficients are introduced. The design value of the coefficients of torsional stiffness reduction for verification of the serviceability limit state (SLS), with assumption of normal probability distribution is determined. The same coefficient is calculated using recommendation for torsional stiffness reduction in concrete elements defined by Model code CEB-FIB 1990 (MC 90). According to conducted analyses the design value of the coefficient of torsional stiffness reduction for verification of the serviceability limit state of main structural elements of beam and slab bridge deck is proposed.*

**Keywords:** Beam and slab bridge deck, Torsional stiffness, SLS.

### 1. Introduction

One of the key solutions to bridging problems in the short and medium span range (10-40 m) is beam and slab bridge deck structure [1-4]. Generally, beam and slab bridge deck is composed of longitudinal beams fitted for prefabrication, cast-in-place transverse beams in the span and over the supports and deck slab composed with longitudinal beams. The main load-carrying components of a beam and slab deck are the longitudinal spanning beams. Transverse distribution of traffic load asymmetric to the longitudinal axis of the bridge to the longitudinal beams is a key quantity in designing new bridges and evaluating existing bridges [1].

In the case of bridge decks with transverse beams in the span and over the supports the transverse load distribution depends mostly on bending stiffness of transverse beams [5,6]. In many bridges the transverse beams in the span are omitted for reasons of simplicity of bridge deck construction. Bridge decks with no transverse beam(s) in the span have less effective but still important transverse distribution achieved by transverse beams over the supports and deck slab. In this case a torsional stiffness

of main structural elements (longitudinal and transverse beams and deck slab) has a great influence on transverse load distribution [1]. However, it should be remember that the torsional stiffness of a concrete element decreases drastically once cracking occurs. Thus, often it will be prudent to reduce the contribution from the torsional stiffness on transverse load distribution.

In the literature, there is very few information about the reduction of torsional stiffness which have to be used in calculation of action effect for ultimate limit state (ULS) and serviceability limit state (SLS) of concrete elements. Authors Pollai and Menon [7] defined that the post-cracking torsional stiffness is only a small fraction (less than 10%) of the pre-cracking stiffness. In Designers' guide to EN 1992-2 [8] it is stated that in the cases where torsional stiffness is considered in analysis, it is important to evaluate it realistically (the cracked stiffness in torsion is typically only about quarter of the uncracked stiffness value). Australian Standards AS5100 [9] reported that the reduction in torsional stiffness of cracked element in relation to uncracked one can be decreased up to 90%. It does say to use no more than 20% of the uncracked torsional stiffness to account for the loss of stiffness after cracking has occurred. Priestley et al [10] suggested that torsional stiffness of cracked elements for superstructure bridge analyses, without the more detailed torsional stiffness calculation can be taken as 5% of uncracked stiffness. MC 90 [11] gives more detailed recommendation

\* Corresponding author: istimac@uniri.hr

<sup>1</sup> Associate professor, PhD Structural Engineering, Radmile Matejčić 3, 51000 Rijeka, Croatia



the deck can be treated as fully continuous for traffic and composite loads. Every span structure consist of six prefabricated longitudinal beams, cast-in-place transverse beams over the supports and cast-in-place deck slab (Fig. 2). Measured deflections determined according to [23] due to asymmetric loading placed in corridor I in the first and in the second span are presented in Table 2.

**Table 2** Measured deflection in the middle of the loaded span on the Slakovci bridge [mm]

Loaded span	Measuring point		
	A	B	C
1 <sup>st</sup>	2.1	1.7	1.0
2 <sup>nd</sup>	3.15	2.7	1.7

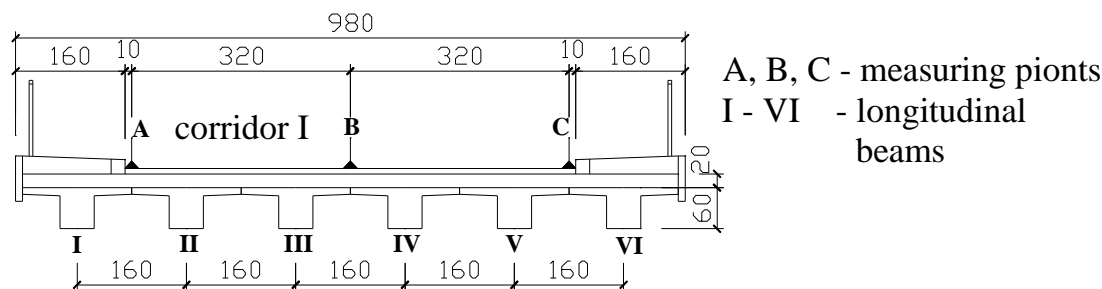


**Fig. 2** The Slakovci bridge cross-section

### 2.3. The Vinično bridge

The bridge is situated on highway route Zagreb – Varaždin – Goričan, sector Komin – Breznički Hum [24].

It is an 8 span structure. Every span structure consist of six prefabricated prestressed longitudinal beams, cast-in-place transverse beams over the supports and cast-in-place deck slab (Fig. 3).

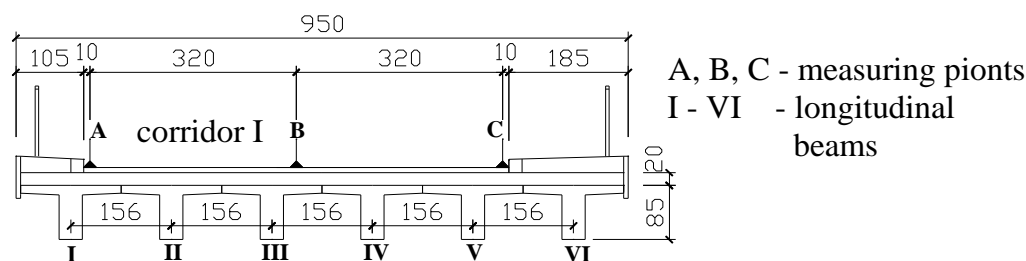


**Fig. 3** The Vinično bridge cross-section

The deck continuity is provided only by the slab over intermediate supports. The axial distances of bridge supports are  $14.51 + 5 \times 18.00 + 14.76 + 14.51$  m. In static sense the span structure is composed of 8 simply supported grillages of span length of 14.30 m in the 1<sup>st</sup>, the 7<sup>th</sup> and the 8<sup>th</sup> span and of 17.54 m in the 2<sup>nd</sup> to the 6<sup>th</sup> spans. The displacements due to asymmetric loading in corridor I placed in the first and in the third span were measured [24]. Measured deflections for these two loading phases are presented in Table 3.

**Table 3** Measured deflection in the middle of the loaded span on the Vinično bridge [mm]

Loaded span	Measuring point		
	A	B	C
1 <sup>st</sup>	2.75	1.3	0.55
3 <sup>rd</sup>	5.55	3.55	2.1

### 2.4. The Brod bridge

The bridge is crossing the river Sava near Slavonski Brod. The bridge is composed of two main structural deck systems: the main steel truss bridge over the river Sava and the concrete approach viaducts [25]. Only the concrete deck structures of approach viaduct (the south viaduct, the central viaduct and the north viaduct) will be analysed in this paper. The south viaduct is a two span structure ( $2 \times 30.00$  m), the central viaduct is a six span structure ( $23.15 + 4 \times 28.50 + 23.15$  m) and the north viaduct is one span structure with span length of 29.00 m.

The bridge deck cross-section shown in Fig. 4 is the same for all approach viaducts. The bridge deck consists of 4 prefabricated prestressed longitudinal beams, cast-in-place transverse beams over the supports and cast-in-place deck slab. The deck continuity at the south and the central viaduct are established by cast-in-place transverse beams at intermediate supports. In static sense the decks of these two viaducts can be treated as fully continuous for traffic and composite loads.

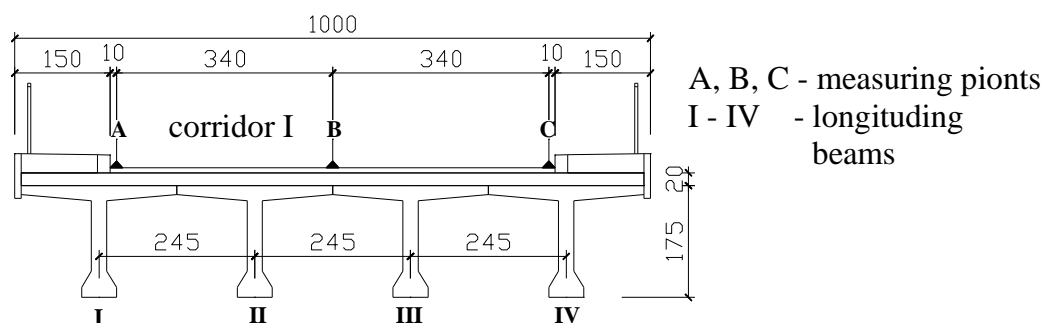


**Fig. 4** The Brod bridge cross-section

In Tables 4, 5 and 6 the measured deflections in the middle of the loaded span determined from [25] for several asymmetrical loading phases on approach viaducts of Brod bridge are shown.

**Table 4** Measured deflection in the middle of the loaded span on the south viaduct of Brod bridge [mm]

Loaded span	Measuring point		
	A	B	C
1 <sup>st</sup>	4.8	3.35	1.2

**Table 5** Measured deflection in the middle of the loaded span on the central viaduct of Brod bridge [mm]

Loaded span	Measuring point		
	A	B	C
1 <sup>st</sup>	2.25	1.65	0.4
3 <sup>rd</sup>	3.4	2.5	1.1

**Table 6** Measured deflection in the middle of the loaded span on the north viaduct of Brod bridge [mm]

Loaded span	Measuring point		
	A	B	C
1 <sup>st</sup>	4.35	3.45	1.55

### 2.5. The Golubinjak bridge

The bridge is situated on highway route Rijeka – Zagreb, sector Vrata – Delnice [26]. The bridge is composed of nineteen simply supported grillage structures of structural span length of 28.90 m. The bridge deck is made up of 4 prefabricated prestressed longitudinal beams, cast-in-place transverse beams over the supports and cast-in-place deck slab (Fig. 5).

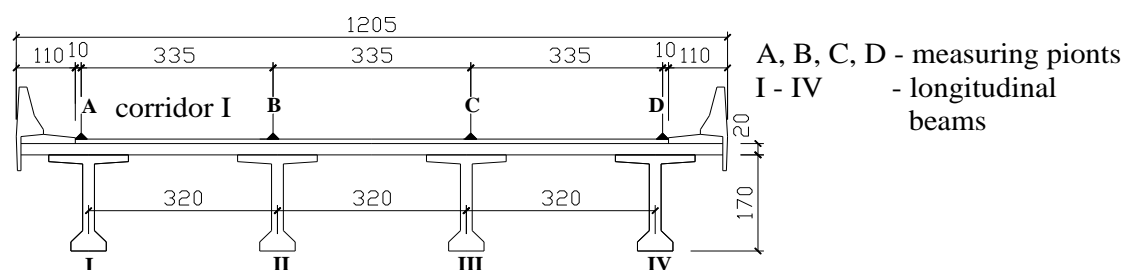


**Fig. 5** The Golubinjak bridge cross-section

The axial distances of bridge supports are 29.50 + 17 x 30.00 + 29.50 m. The deck continuity is provided only by the slab over intermediate supports. Measured deflections determined according to [26] due to asymmetric loading placed in corridor I in the 11<sup>th</sup> and in the 14<sup>th</sup> span are shown in Table 7.

**Table 7** Measured deflection in the middle of the loaded span on the Golubinjak bridge [mm]

Loaded span	Measuring point			
	A	B	C	D
11 <sup>th</sup>	6.0	3.8	2.4	0.7
14 <sup>th</sup>	5.8	4.15	2.0	0.6

### 3. Numerical Models

Theoretical deflections are calculated on appropriate

numerical grillage model of each tested bridge. For the purpose of validation of the measured deflections each numerical model is loaded with the load which corresponds to asymmetric loading scheme applied in load testing. The position of trucks, truck scheme and axle weight are defined in [22-26]. Material and geometric properties of the main structural elements (longitudinal and transverse beams and slabs) are determined according to design documentation.

Theoretical deflections were calculated for each tested bridge by using five numerical models. Numerical models differ only in value of torsional stiffness of finite elements which represents longitudinal and transverse beams and slab. In this paper, torsional stiffness is represented by torsional moments of inertia,  $I_t$ . This can be done in the case where the whole element has the same material property as it is the case in analysed bridges. Torsional

moments of inertia,  $I_t$ , for each numerical model is presented by using basic torsional moment of inertia,  $I_{t0}$  (Table 8). Basic torsional moment of inertia  $I_{t0}$  is determined according to elements dimension taken from the design documentation.

**Table 8** Torsional moment of inertia

Model	1	2	3	4	5
Torsional moment of inertia, $I_{t0}$	$2I_{t0}$	$1.5I_{t0}$	$I_{t0}$	$0.5I_{t0}$	0

The theoretical deflections are calculated for all analysed bridges on described numerical models in the middle of the span(s) in points which correlate with longitudinal beam axis.

### 3.1. The Jamnica bridge

The bridge deck is modelled as a simply supported grillage for each span. It is composed of four longitudinal beams, two transverse beams over supports and 13 transverse beams which represent deck slab (Table 9).

**Table 9** Section properties of the Jamnica bridge model

Element	Area $A [m^2]$	Moment of inertia $I [m^4]$	Basic torsional moment of inertia $I_{t0} [m^4]$	Young's modul of elasticity $E [kN/m^2]$	Poisson's ratio $\nu$
Longitudinal beam	1.1302	0.38207	0.01746	34 000 000	0.2
Transverse beam	0.7212	0.16423	0.0158	31 500 000	0.2
Slab	0.663	0.00773	0.02787	31 500 000	0.2

The numerical model is shown in Fig. 6. The theoretical deflections in the middle of the span are presented in Table 10.

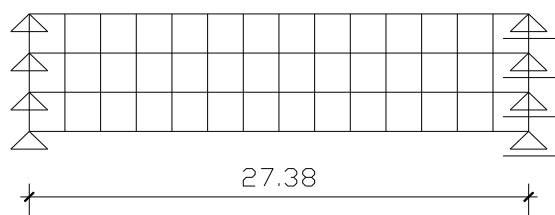


**Fig. 6** The numerical model of the Jamnica bridge

### 3.2. The Slakovci bridge

The bridge deck is modelled as a continuous grillage over 4 spans. Every span is composed of four longitudinal beams and 9 transverse beams which represent deck slab

(Table 11). Five transverse beams are placed over the supports. The numerical model is shown in Fig. 7. The theoretical deflections in the middle of the first span for loading placed in the first span and the theoretical deflections in the middle of the second span for loading in the second span are presented in Tables 12 and 13, respectively.

**Table 10** Theoretical deflection on the Jamnica bridge [mm]

Model	Longitudinal beam			
	I	II	III	IV
1	8.02	6.62	4.71	2.80
2	8.39	6.75	4.60	2.42
3	8.89	6.93	4.45	1.91
4	9.60	7.19	4.23	1.18
5	10.71	7.57	3.88	0.06

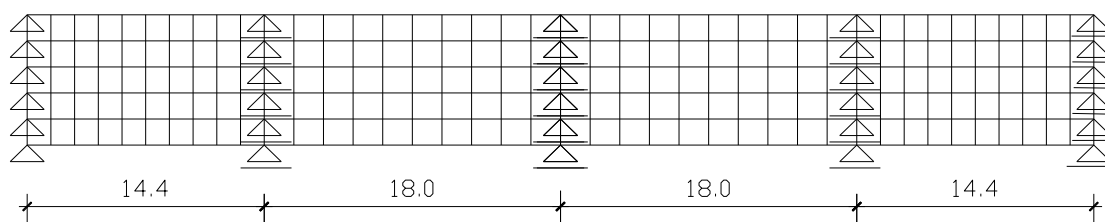


**Fig. 7** The numerical model of the Slakovci bridge

**Table 11** Section properties of the Slakovci bridge model

Element	Area $A [m^2]$	Moment of inertia $I [m^4]$	Basic torsional moment of inertia $I_{t0} [m^4]$	Young's modul of elasticity $E [kN/m^2]$	Poisson's ratio $\nu$
Longitudinal beam					
- in the span	0.7410	0.0351	0.0337	34 000 000	0.2
- over the mid support	1.0105	0.0361	0.0935	34 000 000	0.2
- over the end support	1.2800	0.0683	0.1876	34 000 000	0.2
Transverse beam	0.320	0.0170	0.0710	34 000 000	0.2
Slab					
- in the central spans	0.5580	0.00447	0.0156	34 000 000	0.2
- in the end spans	0.4464	0.00357	0.0123	34 000 000	0.2

Table 12 Theoretical deflection in the first span on the Slakovci bridge [mm]						
Model	Longitudinal beam					
	I	II	III	IV	V	VI
1	3.56	3.59	3.34	2.82	2.35	2.05
2	3.65	3.68	3.39	2.81	2.27	1.91
3	3.80	3.82	3.47	2.79	2.15	1.67
4	4.07	4.07	3.63	2.78	1.92	1.23
5	5.08	4.89	4.11	2.73	1.19	0.32

Table 13 Theoretical deflection in the second span on the Slakovci bridge [mm]						
Model	Longitudinal beam					
	I	II	III	IV	V	VI
1	5.21	5.17	4.82	4.16	3.55	3.12
2	5.36	5.29	4.89	4.15	3.44	2.91
3	5.60	5.48	5.00	4.12	3.26	2.58
4	6.06	5.83	5.18	4.07	2.93	1.95
5	7.89	7.09	5.77	3.85	1.75	0.33

### 3.4. The Vinično bridge

The bridge deck is modelled as a simply supported grillage with six longitudinal beams, two transverse beams over the supports and nine transverse beams which represent deck slab in every span (Table 14). The 1<sup>st</sup>, the 7<sup>th</sup> and the 8<sup>th</sup> spans are modelled with span length of 14.30

m (Model B in Fig. 8), and the 2<sup>nd</sup> to the 6<sup>th</sup> spans with span length of 17.54 m (Model A in Fig. 8). In Table 15, the theoretical deflections in the middle of the span calculated on model A are shown. The theoretical deflections in the middle of the span calculated on Model B are shown in Table 16.

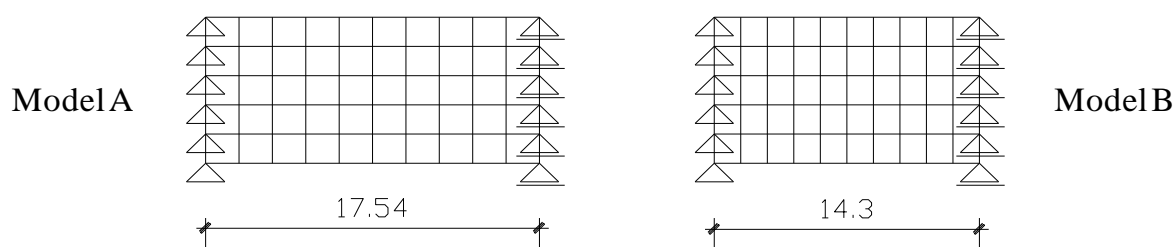


Fig. 8 The numerical models of the Vinično bridge

Table 14 Section properties of the Vinično bridge models A and B					
Element	Area $A [m^2]$	Moment of inertia $I [m^4]$	Basic torsional moment of inertia $It_0 [m^4]$	Young's mod of elasticity $E [kN/m^2]$	Poisson's ratio $\nu$
Longitudinal beam	0.76	0.062	0.0209	34 000 000	0.2
Transverse beam	0.693	0.060	0.0230	31 500 000	0.2
Slab	0.4385	0.0017	0.00817	31 500 000	0.2
-Model A	0.3575	0.0014	0.00639	31 500 000	0.2
-Model B					

Table 15 Calculated deflection on Model A of the Vinično bridge [mm]						
Model	Longitudinal beam					
	I	II	III	IV	V	VI
1	6.70	6.23	5.29	4.05	3.06	2.44
2	7.04	6.46	5.39	3.98	2.83	2.08
3	7.54	6.80	5.52	3.87	2.50	1.54
4	8.36	7.32	5.72	3.72	1.99	0.66
5	9.99	8.31	6.11	3.48	1.04	-1.15

**Table 16** Theoretical deflection on Model B of the Vinično bridge [mm]

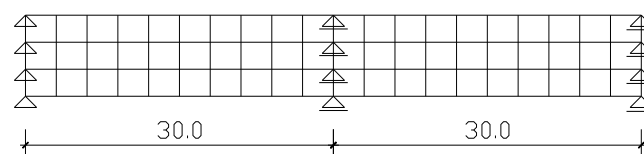
Model	Longitudinal beam					
	I	II	III	IV	V	VI
1	3.47	3.34	2.73	1.85	1.24	0.91
2	3.63	3.47	2.79	1.81	1.12	0.73
3	3.83	3.65	2.87	1.76	0.96	0.48
4	4.12	3.90	3.00	1.70	0.73	0.10
5	4.56	4.31	3.24	1.62	0.38	-0.59

### 3.5. The brod Bridge

#### 3.5.1. The south viaduct of the Brod bridge

The bridge deck is modelled as a continuous grillage over 2 spans. Every span is composed of four longitudinal beams, 9 transverse beams which represent deck slab and the transverse beams placed over the supports (Table 17). The numerical model is shown in Fig. 9. In Table 18, the theoretical deflections in the middle of the first span for

loading placed in the first span are presented.

**Fig. 9** The numerical model of the south viaduct of the Brod bridge**Table 17** Section properties of the south viaduct model

Element	Area $A$ [m <sup>2</sup> ]	Moment of inertia $I$ [m <sup>4</sup> ]	Basic torsional moment of inertia $I_{t0}$ [m <sup>4</sup> ]	Young's modul of elasticity $E$ [kN/m <sup>2</sup> ]	Poisson's ratio $\nu$
Longitudinal beam	1.2488	0.4777	0.0367	34 000 000	0.2
Transverse beam					
- over the mid support	11.74	0.6907	0.2831	31 500 000	0.2
- over the end support	2.58	0.9938	0.8156		
Slab	0.865	0.007365	0.02906	31 500 000	0.2

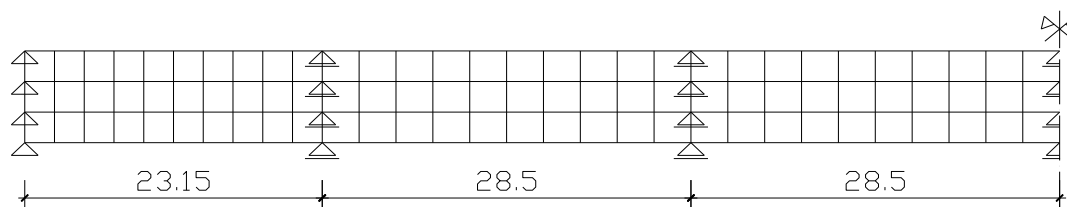
**Table 18** Calculated deflection in the first span on the south viaduct of the Brod bridge [mm]

Model	Longitudinal beam			
	I	II	III	IV
1	6.51	5.59	4.02	2.63
2	6.77	5.69	3.95	2.35
3	7.16	5.83	3.83	1.93
4	7.82	6.08	3.62	1.23
5	9.33	6.62	3.16	-0.36

#### 3.5.2. The central viaduct of the Brod bridge

The bridge deck is modelled as a continuous grillage over 6 spans. Every span is composed of four longitudinal beams, 9 transverse beams which represent deck slab and transverse beams placed over the supports (Table 19). The

numerical model is represented in Fig. 10. The theoretical deflections in the middle of the first span for loading placed in the first span and the theoretical deflections in the middle of the third span for loading in the third span are shown in Tables 20 and 21, respectively.

**Fig. 10** The numerical model of the central viaduct of the Brod bridge**Table 19** Section properties of the central viaduct model

Element	Area $A$ [m <sup>2</sup> ]	Moment of inertia $I$ [m <sup>4</sup> ]	Basic torsional moment of inertia $I_{t0}$ [m <sup>4</sup> ]	Young's modul of elasticity $E$ [kN/m <sup>2</sup> ]	Poisson's ratio $\nu$
Longitudinal beam	1.2484	0.4777	0.0367	34 000 000	0.2

Transverse beam	11.74	0.6907	0.2831	31 500 000	0.2
- over the mid support	2.58	0.9938	0.8156		
- over the end support					
Slab	0.692	0.005891	0.02257	31 500 000	0.2
- in the central spans	0.836	0.0071	0.02726		
- in the end spans					

**Table 20** Calculated deflection in the first span on the central viaduct of the Brod bridge [mm]

Model	Longitudinal beam			
	I	II	III	IV
1	2.89	2.57	1.64	0.94
2	3.00	2.63	1.61	0.81
3	3.15	2.70	1.57	0.63
4	3.39	2.82	1.51	0.33
5	3.85	3.05	1.39	-0.24

**Table 21** Calculated deflection in the third span on the central viaduct of the Brod bridge [mm]

Model	Longitudinal beam			
	I	II	III	IV
1	4.15	3.54	2.35	1.32
2	4.30	3.61	2.31	1.15
3	4.51	3.69	2.25	0.92
4	4.85	3.83	2.14	0.53
5	5.58	4.11	1.93	-0.26

### 3.5.2. The north viaduct of the Brod bridge

The bridge deck is modelled as a simply supported grillage with four longitudinal beams, two transverse beams over supports and nine transverse beams which simulated deck slab (Table 22). The numerical model is shown in Fig. 11. In Table 23, there are listed the theoretical deflections in the middle of the span.

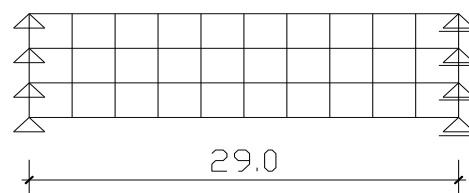


**Fig. 11** The numerical model of the north viaduct of the Brod bridge

**Table 22** Section properties of the north viaduct model

Element	Area $A [m^2]$	Moment of inertia $I [m^4]$	Basic torsional moment of inertia $I_{t0} [m^4]$	Young's mod of elasticity $E [kN/m^2]$	Poisson's ratio $\nu$
Longitudinal beam	1.2488	0.4777	0.0367	34 000 000	0.2
Transverse beam	1.74	0.6907	0.2831	31 500 000	0.2
Slab	0.865	0.007365	0.02966	31 500 000	0.2

**Table 23** Calculated deflection on the north viaduct of the Brod bridge [mm]

Model	Longitudinal beam			
	I	II	III	IV
1	7.96	6.90	5.20	3.67
2	8.30	7.03	5.09	3.30
3	8.83	7.23	4.92	2.74
4	9.77	7.56	4.63	1.76
5	11.86	8.30	3.98	-0.42

### 3.6 The Golubnjak bridge

The bridge deck is modelled as a simply supported grillage with four longitudinal beams, two transverse beams over supports and five transverse beams which simulated deck slab (Table 24). The numerical model is shown in Fig. 12. The theoretical deflections in the middle of the span are listed in Table 25.

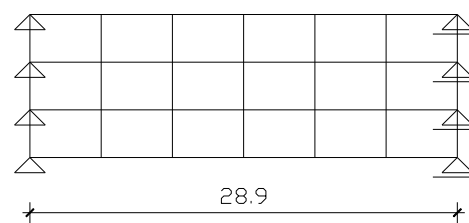


**Fig. 12** The numerical model of the Golubnjak bridge



**Table 24** Section properties of the Golubinjak bridge model

Element	Area $A \text{ [m}^2\text{]}$	Moment of inertia $I \text{ [m}^4\text{]}$	Basic torsional moment of inertia $It_0 \text{ [m}^4\text{]}$	Young's modul of elasticity $E \text{ [kN/m}^2\text{]}$	Poisson's ratio $\nu$
Longitudinal beam	1.1338	0.456375	0.0347866	32 750 000	0.2
- mid beam	1.2338	0.477631	0.0346211		
- edge beam					
Transverse beam	0.7380	0.20648	0.015930	31 500 000	0.2
Plate	0.7380	0.20648	0.017261	31 500 000	0.2

**Table 25** Calculated deflection on the Golubinjak bridge [mm]

Model	Longitudinal beam			
	I	II	III	IV
1	9.38	6.95	3.78	1.68
2	9.76	7.06	3.65	1.32
3	10.27	7.21	3.48	0.84
4	11.02	7.40	3.24	0.13
5	12.47	7.73	2.81	-1.22

#### 4. Comparison of Transverse Deflection Distribution

The transverse distribution coefficients are introduced to simplify the analysis. Generally, the transverse distribution coefficient  $\alpha$  represents deviation of middle span deflection at measuring point nearest to the loaded bridge edge to a mean value of middle span deflection for asymmetric bridge loading. The transverse distribution coefficient  $\alpha_m$  represents deviation of measured middle span deflection at measuring point A to a mean value of measured middle span deflection at all measuring points in

the bridge cross section and the transverse distribution coefficient  $\alpha_t$  represents deviation of theoretical middle span displacement at measuring point A to a mean value of theoretical middle span deflection at all longitudinal beams in the bridge cross section. The value of theoretical deflection which corresponds with position of measuring point A is determined by using linear interpolation between the theoretical deflections calculated in the longitudinal beams axes nearest to the measuring point A. The values of transverse deflection distribution  $\alpha_m$  and  $\alpha_t$  are shown in Table 26.

**Table 26** The transverse distribution coefficients  $\alpha$ 

No.	Bridge	Loaded span	$\alpha_m$	$\alpha_t$				
				Model 1	Model 2	Model 3	Model 4	Model 5
1	Jamnica	1st	1.44	1.43	1.49	1.58	1.70	1.88
2		3rd	1.52	1.43	1.49	1.58	1.70	1.88
3	Slakovci	1st	1.31	1.21	1.24	1.29	1.38	1.63
4		2nd	1.25	1.20	1.23	1.28	1.37	1.68
5	Vinično	1st	1.8	1.53	1.59	1.68	1.81	2.00
6		3rd	1.49	1.43	1.50	1.60	1.76	2.09
7	Brod -south	1st	1.54	1.37	1.42	1.50	1.63	1.93
8	Brod - central	1st	1.57	1.42	1.47	1.54	1.66	1.88
9		3rd	1.46	1.44	1.49	1.56	1.67	1.91
10	Brod - north	1st	1.39	1.32	1.38	1.46	1.61	1.94
11	Golubinjak	11th	1.86	1.75	1.82	1.92	2.06	2.34
12		13th	1.85	1.75	1.82	1.92	2.06	2.34

The ratio  $\alpha_m/\alpha_t$  describes deviation of transverse displacement distribution for tested bridge and a numerical model. The ratios  $\alpha_m/\alpha_t$  were calculated for  $It/It_0=2$  (Model 1),  $It/It_0=1.5$  (Model 2),  $It/It_0=1.0$  (Model 3),  $It/It_0=0.5$  (Model 4),  $It/It_0=0$  (Model 5) and are shown in Table 27. Linear interpolation can be employed to get values  $\alpha_m/\alpha_t$  for other torsional stiffness ratios.

Using this fact it is easy to determine the value of

torsional stiffness ratio  $k_t$  which has to be used in numerical model to satisfy the criterion of the equality of transverse displacement distribution for tested bridge and the numerical model. The values  $k_t = It/It_0$  for  $\alpha_m/\alpha_t = 1$  are determined by using linear interpolation between calculated ratios shown in Table 27. The values  $k_t$  are shown in Table 28.

**Table 27** The ratios  $\alpha_m/\alpha_t$ 

No.	Bridge	Loaded span	$\alpha_m/\alpha_t$				
			Model 1	Model 2	Model 3	Model 4	Model 5
1	Jamnica	1 <sup>st</sup>	1.01	0.97	0.91	0.85	0.77
2		3 <sup>rd</sup>	1.06	1.02	0.96	0.89	0.81
3		1 <sup>st</sup>	1.08	1.06	1.02	0.95	0.80
4	Slakovci	2 <sup>nd</sup>	1.04	1.02	0.98	0.91	0.74
5		1 <sup>st</sup>	1.18	1.13	1.07	0.99	0.90
6	Vinično	3 <sup>rd</sup>	1.04	0.99	0.93	0.85	0.71
7		1 <sup>st</sup>	1.12	1.08	1.03	0.94	0.80
8	Brod - south	1 <sup>st</sup>	1.11	1.07	1.02	0.95	0.84
9		3 <sup>rd</sup>	1.01	0.98	0.94	0.87	0.76
10	Brod - north	1 <sup>st</sup>	1.05	1.01	0.95	0.86	0.72
11		11 <sup>th</sup>	1.06	1.02	0.97	0.90	0.79
12	Golubinjak	13 <sup>th</sup>	1.06	1.02	0.96	0.90	0.79

**Table 28** The torsional stiffness ratio  $k_t$ 

No.	1	2	3	4	5	6	7	8	9	10	11	12
$k_t$	1.88	1.33	0.86	1.25	0.56	1.60	0.83	0.86	1.83	1.42	1.3	1.33

For some bridges, it is determined that the real torsional stiffness of elements is greater than the basic torsional stiffness. The reasons for this behaviour may be different: (a) the dimensions of constructed elements may be greater than the ones in the project documentation, especially slab thickness; (b) the deviation of the truck position in the testing and in the numerical model, (c) the stiffness of non-structural elements which are not taken into analysis (pavement, concrete fences, asphalt...) is not included in numerical modelling.

## 5. Evaluation

The design value of the coefficients of torsional stiffness reduction for serviceability limit state (SLS),  $k_{td}$ , will be determined. The design value of the coefficients of torsional stiffness reduction with assumption of normal probability distribution for huge number ( $n > 30$ ) of independent measured data can be derived from next equation [27]:

$$X_d = \mu - \alpha_R \cdot \beta \cdot \sigma \quad (1)$$

where:

$X_d$  – is the design value

$\mu$  – is the mean value of independent data based on the population

$\alpha_R$  – is the sensitivity factor for resistance

$\beta$  – is the reliability index

$\sigma$  – is the standard deviation of independent data based on a population.

When a small number of independent data (in the considered case  $n = 12$ ) is available to predict the design value a standard Bayesian prediction formula can be used [27]:

$$X_d = m - t_v \cdot \sqrt{\left(1 + \frac{1}{n}\right)} \cdot s_n \quad (2)$$

where:

$m$  – is the mean value of independent data based on the sample

$s_n$  – is the standard deviation of independent data based on the sample

$n$  – is the number of independent data

$t_v$  – is the value for Student's  $t$  – distribution for  $v$  degrees of freedom and chosen fractile

$v$  – is the number of degrees of freedom ( $v = n - 1$ ).

If it is assumed that  $n = \infty$  the following equation can be derived from the Equations (1) and (2):

$$t_v = \alpha_R \cdot \beta \quad (3)$$

The target value for reliability index  $\beta$  for SLS and for reference period of 50 years is 1,5 [28]. The value of the sensitivity factor for the uncertain basis variable for resistance,  $\alpha_R$ , determined according to EN 1990 is 0,8 [27]. The uncertain basis variable in this case represents modal uncertainties (uncertainties of torsional stiffness).

The fractile of 11.7 % is determined by using Student's  $t$  – distribution for  $v = \infty$  and  $t_v = 0.8 \cdot 1.5 = 1.2$ .

The value of Student's  $t$  – distribution for  $v = 12 - 1 = 11$  degrees of freedom and determined fractile of 11.7% is  $t_v = 1.27$ .

Now, the design value of the coefficients of torsional stiffness reduction for serviceability limit state (SLS),  $k_{td}$ , for  $n=12$  independent data (Table 28), can be determined according to next equation:

$$k_{td} = k_{tm} - t_v \cdot \sqrt{\left(1 + \frac{1}{n}\right)} \cdot k_{ts} \quad (4)$$

where:

$k_{tm}$  – is the mean value of independent data  $k_t$  (from Table 28)

$k_{ts}$  – is the standard deviation of independent data  $k_t$  (from Table 28).

$$k_{td} = 1.25 - 1.27 \cdot \sqrt{\left(1 + \frac{1}{12}\right)} \cdot 0.41 = 0.71$$

The design value of the coefficients of torsional stiffness reduction for serviceability limit state (SLS) [27]  $k_{td}$  is 0.71.

On the basis of the testing results, applied testing loads and according to the fact that longitudinal beams are prestressed it can be concluded that no cracks occur in elements during the testing.

According to Model code CEB-FIB 1990 (MC 90) [11] the torsional stiffness  $K$  per unit length in stage I (uncracked stage) is defined as follows:

$$K_I = \frac{0.3 \cdot E_{cm} \cdot I_{t0}}{1 + 1 \cdot \varphi} \quad (5)$$

where:

$E_{cm}$  – is the modulus of elasticity of concrete

$I_{t0}$  – is the torsional moment of inertia in uncracked stage

$\varphi$  – is the creep coefficient to be used for long term loading.

The creep coefficient for short-term testing is  $\varphi = 0$ . According to this fact the equation (5) turns to:

$$K_I = 0.30 E_{cm} \cdot I_{t0} \quad (6)$$

The torsional stiffness per unit length according to the theory of strength of material is:

$$K_t = G \cdot I_{t0} \quad (7)$$

Using analogy in Equations (6) and (7) it can be seen that in MC 90

$$0.3 \cdot E_{cm} = G \quad (8)$$

As it is known from the theory of concrete structures, the shear modulus is approximately determined as  $G = 0.4 E_{cm}$ . This value is greater than the one in Equation (8). Based on this consideration it is obvious that MC 90 has introduced the torsional stiffness reduction even for uncracked elements. In MC 90 [11], there is a quotation: "In the expression for  $K_I$  the factor 0.30 takes account of the non-linear behaviour of concrete before cracking." It leads to the conclusion that the design value of the coefficients of torsional stiffness reduction for uncracked elements according to MC 90 is  $k_{td}=0.3/0.4=0.75$ . This value is greater than the value got from conducted analysis based on bridge field test ( $k_{td}=0.71$ ).

On the basis of results obtained from on-site testing compared to results taken from numerical models and comparison to recommendation taken from MC90 authors propose design value of the coefficients of torsional stiffness reduction for serviceability limit state (SLS) as  $k_{td}=0.71$ .

## 6. Conclusion

In this paper the design value of the coefficient of torsional stiffness reduction for verification of the serviceability limit state based on experimental research conducted on series of beam and slab bridge decks is determined. This value is compared with the design value of the coefficient of torsional stiffness reduction recommended by MC90. According to conducted comparative analyses the design value of the coefficients of torsional stiffness reduction for verification of the serviceability limit state is proposed.

## References

- [1] Yousif Z, Hindi R. AASHTO-LRFD live load distribution for beam-and-slab bridges: limitation and applicability, *Journal of Bridge Engineering*, 2007.
- [2] Hastak M, Mirmiran A, Miller R, Shah R, Castrodale R. State of practice for positive moment connections in prestressed concrete girders made continuous, *Journal of Bridge Engineering*, No. 5, Vol. 8, 2003, pp. 267-272.
- [3] Taylor HHJ. The precast concrete beam: the first 50 years, *The structural engineer*, No. 21, Vol. 76, 1997, pp. 407-414.
- [4] O'Brien EJ, Keogh DL. *Bridge Deck Analysis*, Taylor & Francis group, London, 2005
- [5] Ardalić Z. Valorization of various grillage models based on field tests of the underpass Vrata 1, Thesis, Rijeka, 2011, in Croatian.
- [6] Latić V. Experimental determination of torsional stiffness in ribbed bridge deck, Thesis, Rijeka, 2009, in Croatian.
- [7] Pillai SU, Menon D. *Reinforced Concrete Design*, Tata McGraw-Hill Publishing Company Limited, New Delhi, 2003.
- [8] Hendy CR, Smith DA. *Designers' guide to EN 1992-2 Eurocode 2: Design of Concrete structures, Part 2: Concrete bridges*, Tomas Telford Ltd, London, 2007
- [9] AS 5100 Australian Standards-Bridge Design, Standard Australia International Ltd, Sydney, 2004.
- [10] Priestley MJN, Seible F, Calvi GM. *Seismic Design and Retrofit of Bridges*, John Wiley & Sons INC, New York, 1996.
- [11] CEB-FIB, CEB-FIB Model Code 1990 (MC-90), Design Code, Comité Euro-International du Béton (CEB), Thomas Telford Services Ltd, London, 1993.
- [12] Mondorf PE. *Concrete Bridges*, Taylor and Francis, New York, 2006.
- [13] Kaveha A, Talatahari S. Charged system search for optimum grillage system design using the LRFD-AISC code, *Journal of Constructional Steel Research*, Vol. 66, 2010, pp. 767-771.
- [14] Linzell DG, Shura JF. Erection behavior and grillage model accuracy for a large radius curved bridge, *Journal of Constructional Steel Research*, 2010, Vol. 66, pp. 342-350.
- [15] Qaqish M, Fadda E, Akawwi E. Design of T-beam bridge by finite element method and AASHTO specification, *KMITL Science Journal*, 2008, No. 1, Vol. 8, pp. 24-34.
- [16] Gupta T, Misra A. Effect on support reactions of T-beam skew bridge decks, *ARPJ Journal of Engineering and Applied Sciences*, 2007, No. 1, Vol. 2, pp. 1-8.
- [17] Kakish M. Bending moments distribution at the main structural elements of skew deck-slab and their implementation on cost effectiveness, *American Journal of Applied Sciences*, 2007, No. 12, Vol. 4, pp. 1036-1039.

- [18] Al-Sarraf SZ, Ali AA, Al-Dujaili RA. Analysis of composite bridge superstructures using modified grillage method, *Journal of Engineering and Technology*, 2009, No. 5, Vol. 27, pp. 942-953.
- [19] Nevling D, Linzell D, Laman J. Examination of level of analysis accuracy for curved i-girder bridges through comparisons to field data, *Journal of Bridge Engineering*, 2006, No. 2, Vol. 11, pp. 160-168.
- [20] Amer A, Arockiasamy M. Load distribution of existing solid slab bridges based on field tests, *Journal of Bridge Engineering*, 1999, No. 3, Vol. 4, pp. 189-193.
- [21] Croatian standard, HRN U.M1.046, Experimental load testing of bridges, 1984, in Croatian.
- [22] Load testing report of the bridge over the river Kupa near Jamnička Kiselica on the road R 2117, IGH, Zagreb, 2000, in Croatian.
- [23] Load testing report of the bridge Slakovci – Otok over the river Bosut, IGH, Zagreb, 2001, in Croatian.
- [24] Load testing report of the bridge Vinično over the highway Zagreb – Varaždin – Goričan, section Komin – Breznički Hum from km 28 + 400 to km 40 + 700, IGH, Zagreb, 2000, in Croatian.
- [25] Load testing report of the bridge over the river Sava in Brod, IGH, Zagreb, 2000, in Croatian.
- [26] Load testing report of the bridge Golubinjak on the highway Rijeka – Zagreb, section Vrata – Delnice, km 36 + 949.40, IGH, Zagreb, 1996, in Croatian.
- [27] Probabilistic Assessment of Existing Structures, A Publication of the Joint Committee on Structural Safety (JCSS), France, 2001.
- [28] EN 1990, Eurocode: Basis of structural design, CEN, Bruxelles, 2002.